Proc. 15th INA Conf., Bohol, Philippines
J. Nannoplankton Res. **36** (2), 2016, pp.139–147 © 2016 International Nannoplankton Association
ISSN 1210-8049 Printed by The Sheridan Press, USA

A semi-automatic two-dimensional image system for studying the skeletal design of the silicoflagellate genus *Corbisema* (Dictyochales, Dictyochophyceae)

Hideto Tsutsui* and Richard W. Jordan

Department of Earth and Environmental Sciences, Faculty of Science, Yamagata University, 1-4-12 Kojirakawa-machi, Yamagata 990-8560, Japan; *blacksand@mail.goo.ne.jp

Manuscript received 6th November, 2015; revised manuscript accepted 25th July, 2016.

Abstract Variations in skeletal morphology can provide valuable information on silicoflagellate classification and evolution, as well as the ontogenetic process of skeleton formation; however, measuring hundreds of individual skeletons can be time-consuming, and there are few, if any, existing morphometric programs that can be used to study the triangular skeletons of *Corbisema*. Thus, a morphometric program previously designed to measure *Stephanocha* (= *Distephanus*) spp. was modified to investigate *Corbisema* spp., using *C. apiculata* from Mors, Denmark (early Eocene) as a test case. Although the obtained sample set contains specimens with and without pikes, as well as differences in the pike-strut distance, some basic statements can be made: (1) in general, the basal ring is an isosceles triangle with two equal sides and one slightly shorter side, and (2) radial spine length and basal side length both exhibit a unimodal distribution. The distance between the pike and strut ranges from 0 to 5μm, with a mean distance/skeleton of 0–1μm representing 77% of the total specimens, and that of >2μm representing 3%. This may be related to their double skeleton configuration, with specimens lacking pikes or with large distances between pike and strut possibly associated with a 'corner-to-corner' configuration, while those with pikes close to the struts forming 'Star-of-David' configurations. The taxonomic implications of this result are discussed in relation to the recent literature.

Keywords computer program, *Corbisema apiculata*, Eocene, morphometry, Mors

1. Introduction

1.1 Morphometric studies for plankton and microfossils

In the distant past, measurements of plankton or microfossils were done manually using the microscope graticule or from printed images – a time-consuming process which often deterred the measurement of large numbers of individuals. Later, morphometric procedures like eigenshape analysis (Lohmann, 1983) and automated image capture (Young *et al*., 1996) became useful tools for the microscopist. More recently, over the last decade or so, a number of sophisticated automatic recognition systems like SYRACO (Dollfus & Beaufort, 1999; Beaufort & Dollfus, 2004), COGNIS (Bollmann *et al*., 2004) and AMOR (Knappertsbusch & Schneider, 2009) have been developed which can analyze specimens on microscope slides, speeding up measurements and improving accuracy and reproducibility.

Morphometric techniques using foraminifers, radiolarians, coccolithophores, diatoms, dinoflagellate cysts and pollen have already been discussed in numerous papers (e.g., Pappas & Stoermer, 1995; Cortese & Bjørklund, 1997; Lindbladh *et al*., 2002; Cortese & Gersonde, 2007; Mertens *et al*., 2009; Veselá *et al*., 2009; Aurahs *et al*., 2011; Cubillos *et al*., 2012; Schneider, *et al*., 2012; Siver *et al*., 2013; Rasband, 1997–2013). However, some disadvantages still exist, e.g., system, hardware or software development cost and re-measurement labor.

Some workers have used mathematical models to represent silicoflagellate skeletal designs, noting that more complex designs (e.g., hexagons and heptagons) inhabit higher latitudes and thus cooler temperatures (McCartney & Loper, 1989; 1992). Most *Corbisema* spp. have a triangular outline, but some species like *C. apiculata* have curved basal sides that could be viewed as approximating a circle, which minimizes the apical area (McCartney & Loper, 1992). Some silicoflagellate morphometric studies, for example, noted differences in cell volume using a three-dimensional approach (McCartney, 1988; McCartney & Loper, 1989; 1992), while others demonstrated morphologic diversity and a relationship between radial spine length and environmental conditions based on the skeletal form as a two-dimensional, computerized wire-frame model (Tsutsui *et al*., 2009; Tsutsui & Takahashi, 2009). These latter studies used a landmark-based geometric morphometrics program (Tsutsui, 2000) to calculate element lengths and angles at designated landmarks (i.e., with coordinates) present on all of the selected specimens.

1.2 Silicoflagellate taxonomy

Silicoflagellates are unicellular marine phytoplankton belonging to the Class Dictyochophyceae (see recent review by Jordan *et al*., submitted) and form a monophyletic clade within the class according to recent molecular phylogeny data (Chang *et al*., 2012). However, there is still

controversy about how many extant genera and species exist; many biologists believe that all extant species belong to only one genus (*Dictyocha*; e.g., Moestrup & Thomsen, 1990; Chang, 2015), whilst most micropaleontologists think that the evolutionary trends among fossil taxa support the need for three extant silicoflagellate genera (*Dictyocha*, *Stephanocha* and *Octactis*; e.g., McCartney *et al*., 2014a; 2014b – the illegitimate genus *Distephanus* was recently replaced by the new genus *Stephanocha*; Jordan & McCartney, 2015). The classification of fossil species is more complicated, since generic concepts tend to be based on small morphological differences, and the full range of skeletal plasticity (including aberrants) within a single taxon is difficult to document. In general, Cenozoic genera can be separated by shape; two-sided (*Naviculopsis*), triangular (*Corbisema*), quadrangular (*Dictyocha* and *Distephanopsis*), hexagonal (*Stephanocha*), octagonal (*Octactis*) or polygonal (*Bachmannocena* and *Caryocha*); however, within the same genus the number of basal sides and basal spines can, albeit more rarely, be higher or lower than generally found – thus, five-sided *Dictyocha* or seven-sided *Stephanocha* skeletons may be encountered.

When skeleton-bearing silicoflagellates undergo cell division a second, sometimes thinner skeleton (daughter skeleton) is laid down opposite the original skeleton (mother skeleton) (Marshall, 1934), or the mother skeleton is discarded and two identical skeletons are produced (Chang, 2015). Normally, these skeletons are identical, not mirror-images of each other (cf. Boney, 1976), so that the pikes of the paired skeletons interlock on opposite sides of the strut, or in taxa where pikes are absent, organic material holds the two skeletons together (McCartney *et al*., 2014b). Modern silicoflagellate double skeletons align with basal rings and basal spines closely abutting, in the so-called 'corner-to-corner' configuration, while many Late Cretaceous and Paleogene silicoflagellates employed a different strategy, with one skeleton rotated 180° in a 'Star-of-David' configuration (e.g., McCartney *et al*., 2010; Dumitrica, 2014). So far, all known examples of 'Star-of-David' configurations involve skeletons with pikes (e.g., *Corbisema* and *Dictyocha* – see McCartney *et al*., 2014a, 2014b). Pike positions on single skeletons can be used to determine which configuration a paired skeleton would have adopted, with pikes close to the strut associated with the 'Star-of-David' configuration, and pikes offset from the strut associated with the 'corner-to-corner' configuration.

1.3 Aims

In this paper we use a modified version of a semi-automated morphometric program developed for six-sided *Stephanocha* skeletons to calculate element lengths and angles of three-sided *Corbisema* skeletons, using *C. apiculata* in a sample from Mors, Denmark as a test case. It is hoped that this modification will allow us in the future to solve taxonomic problems in *Corbisema*.

2. Materials and methods

2.1 Geological setting

The Fur Formation on Mors, Denmark (Figure 1) has been studied by scientists for hundreds of years, mainly because of the wealth of marine fossils that have been found there (e.g., Nielsen, 1959; Collins *et al*., 2005), but also for the laminated diatomites, which are well-preserved due to the anoxic conditions that prevailed during their deposition (Pedersen, 1981). These diatomite layers, intercalated with ash deposits (Pedersen & Surlyk, 1983), are thought to be early Eocene in age, based on various microfossil groups (Perch-Nielsen, 1976; Homann, 1991; Fenner, 1994; Jørgensen *et al*., 2005) and volcanic ash radiometric ages of 54.52 +/– 0.05Ma and 54.04 +/– 0.14Ma (Chambers *et al*., 2003). Sedimentological studies also suggested an upper Paleocene-Eocene age for the Fur Formation, with the depositional paleoenvironment interpreted as being marine with some brackish influence well below the wave base (Heilmann-Clausen *et al*., 1985). The present study adopted an early Eocene depositional age of the Fur Formation as suggested previously by Collins *et al*. (2005) and Jørgensen *et al*. (2005).

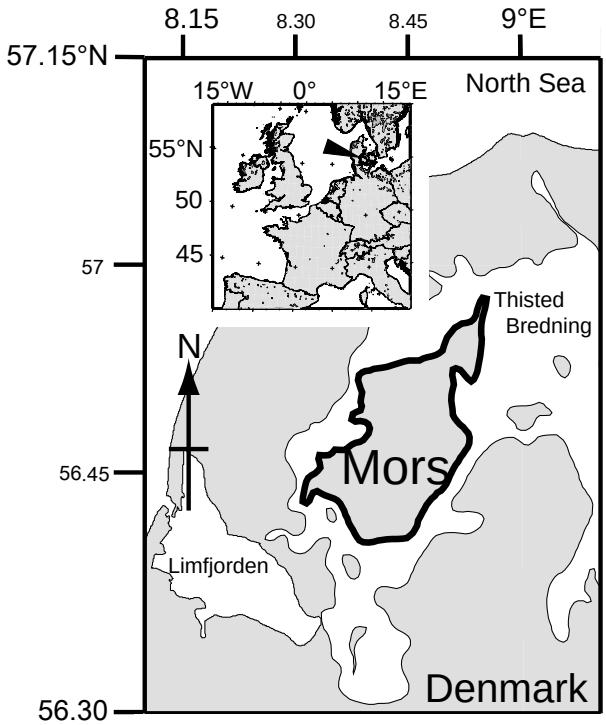

Figure 1: Map of sample location. The *Corbisema* specimens used in this study were in an outcrop sample collected from Mors Island, Denmark. The sample accession number is E1758 and the sample is curated in the Friedrich Hustedt Diatom Study Center at the Alfred-Wegener-Institute, Helmholtz-Zentrum für Polar- und Meeresforschung (AWI), Bremerhaven, Germany. The map was produced using the mapping software of GEOMAR, Collaborative Research Center (SFB) 574. http://www.sfb574.geomar.de/gmt-maps/html

2.2 Silicoflagellate analysis

Silicoflagellates, especially *Corbisema*, are frequent in the Fur Formation, so they make ideal subjects for morphometric analysis. Measurements were carried out on the light microscope because this was the method chosen for previous silicoflagellate morphometric studies and observations can be made quickly. The preparation of permanent mounts follows the method outlined in Shiono & Jordan (1996), with Mountmedia® (Wako Pure Chemical Industries, Ltd.) as the mounting medium (refractive index = >1.50). Specimens were observed using x10, x20 or x40 objective lenses on an Olympus® BH2 and photographed with an AR-D300C digital camera (ARMS System, Co., LTD) or on a BX40 with an NY-1S relay lens (Microscope Network Co., Ltd) and EOS Kiss® X6i camera (Canon, Inc.).

2.3 Morphometric sample selection

The morphometric program requires that the main skeletal parts are not broken; however, the radial spine tip of *Corbisema*, in particular, is very fragile. Before carrying out measurements, the following four conditions must be satisfied: (1) specimens must be photographed in apical or abapical view; (2) specimens must not be tilted, so all radial spine tips or all basal sides should be in the same focal plane; (3) specimens should be 'normal', without the loss or addition of some skeletal parts or obvious deformities (e.g., Loeblich *et al*., 1968; Malinverno, 2010); and (4) specimens must not be partially obscured by debris, making measurement of some skeletal parts impossible. The common forms of *C. apiculata* found in this study are shown in Figure 2a–c, with the parameters to be measured shown in Figure 2d.

The morphometric results and statistics should be supported by a large number of specimens. Fortunately, the Mors sample satisfied the following conditions: (1) good preservation; (2) abundant silicoflagellates, especially of *Corbisema*; and (3) presence of both 'Star-of-David' and 'corner-to-corner' skeletal configurations of *Corbisema*, as already described by McCartney *et al*. (2014a; 2014b; 2015b).

2.4 Measuring program and procedure

The measuring program language and source code run on the freeware interpreter 99BASIC Interpreter Version 1.19 (Iida, 2002), which itself runs on Microsoft® Windows®. The merit of this program is that the main source code can be easily debugged, and the system can be downsized relatively quickly. The primary algorithms, data architectures and program routines are based on the morphometric system of *Stephanocha speculum* (Tsutsui, 2000). The measuring system of this study requires the following two manual input steps: (1) the 8-bit bitmap load on this program, and (2) skeletal end-points, junctions and scale bar length. The basic concept of this morphometric system is based on *Corbisema* specimens with linear basal sides;

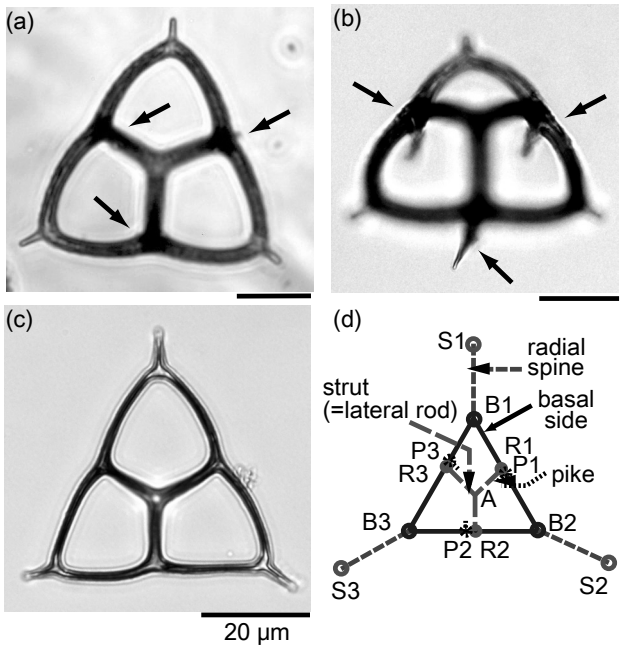

Figure 2: Two skeletal forms of *Corbisema apiculata* and measurement strategy: **(a)** pike-bearing form in apical view; **(b)** pike-bearing form in tilted lateral view. The arrows point to pikes; **(c)** pike-less form; and **(d)** idealized skeleton showing parameters to be measured

however, in reality, those with bulging basal sides can also be measured by applying the Bézier curve system. The Bézier curve is useful for drawing a smooth curve on computer graphics, because it can be expressed with one control point. The Bézier curve calculation method used in our program is based on Forrest (1972). An example of this calculation can be seen in Figure 3, with computer screen shots after loading the microphotograph bitmap (Figure 3a) and of the subsequent measurement result after bitmap loading (Figure 3b).

The calculation time of length, pike distance and angles is instantaneous. The main advantages of this morphometric system are threefold: (1) Re-measurement work is very easy because this program can recalculate the measurement data from the coordinate data, (2) the measurement program can quickly process large amounts of photographic data, and (3) the labor time needed for measuring is reduced.

Another advantage of this program is that it can automatically identify skeletal parts, which can be numbered in a clockwise direction; for instance, in the case of *Corbisema*, the three spines are numbered sequentially, with spines at twelve o'clock (= 1), four o'clock (=2), and eight o'clock (=3). Other skeletal parts (struts, pikes etc) are numbered in the same way.

The actual morphometric steps are as follows: First, the photomicrograph is converted from an image file (such as JPEG or TIFF) to an 8-bit bitmap image, which is reduced in size to 800 × 800 pixels. The program then creates two data files: (1) the X/Y coordinate data on

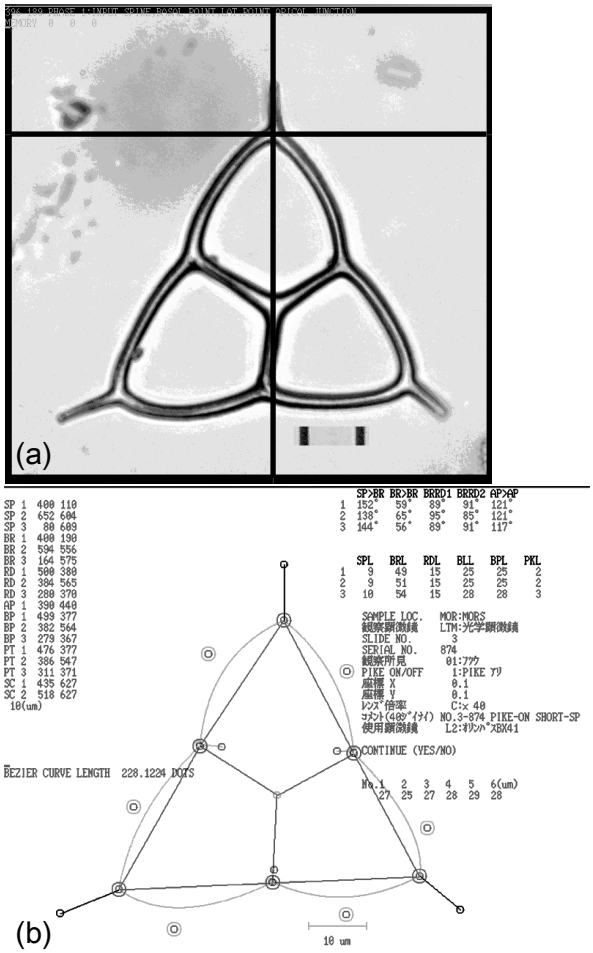

Figure 3: Computer screenshots of coordinate input situation and result output: **(a)** Screen shot after bitmap loading, and **(b)** after the completed procedure. The cross line in 3a is the target for manual input. In 3b the vertical output on the left is the coordinate data, with length, angle, curved length and scale length shown on the right

the computer screen is saved as 'silicoad.ctl' (Table 1), and (2) the morphometric data output as 'silicolw.txt' (Table 2). Two data files of fixed length are outputted in ASCII code. The left portion of Table 1 shows the Sample ID which consists of sample origin, microscope type, slide number, serial photograph number, objective lens, location of sample on the slide and comments. The X/Y coordinate data in Table 1 are listed in clockwise order after the sample ID: radial spines numbered 1 to 3, basal ring corner, strut position, pike position, apex point and curved basal side. The morphometric data in Table 2 consists of the X/Y coordinate of the scale bar, scale bar length, skeletal element length, angles and curved basal side length. A zero means the value is outside the limits of measuring. These files are kept in plain ASCII Character–Separated Values (CSV) format, which is fully compatible with other software (e.g., SAS® by SAS Institute Inc., SPSS® by IBM SPSS Statistics® or Microsoft® Excel®). Consequently, the rewrite and overwrite of file contents can be easily carried out. The statistical data (kurtosis,

Sample logistics (MOR: Mors) and Microscope type (LTM: Light microscope)	Slide ID and serial number	Observation code and pike on-off (1: Normal, 1: Pike-on)	Microscope stage position (X and Y)	Lens type (A: x10 and x5 zoom lens)	Comments	ID area	Microscope machine type (L3: Olympus BX40)	Scale bar start (X and Y)		Scale bar end (X and Y)		Scale bar length (10μm)	Spine 1 (X and Y)		Spine 2 (X and Y)		Spine 3 (X and Y)		Basal corner 1 (X and Y)		Basal corner 2 (X and Y)		Basal corner 3 (X and Y)		Basal-strut junction 1 (X and Y)		Basal-strut junction 2 (X and Y)		Basal-strut junction 3 (X and Y)		Apical junction (X and Y)		Basal pike 1 (X and Y)		Coordinate area
MORLTM	1-159	1,1	0.1, 0.1	A	NO.1-154 PIKE-ON SHORT-SP		L3	85	222	142	222	10	286	45	529	430	60	406	290	105	470	397	114	380	385	246	286	403	205	242	287	314	402	264		
MORLTM	1-160	1,1	0.1, 0.1	A	NO.1-160 SHORT-SP PIKE-ON		L3	206	274	87	274	10	410	40	740	598	60	558	407	113	670	538	160	508	537	318	430	518	320	308	430	368	540	(omit)		
MORLTM	1-161	1,1	0.1, 0.1	A	NO.1-161 SHORT-SP PIKE-ON		L3	358	432	415	432	10	295	70	492	442	95	398	295	100	434	394	129	381	369	245	279	388	206	231	271	285	380	258		
MORLTM	1-166	1,1	0.1, 0.1	A	NO.1-166 SHORT-SP PIKE-ON		L3	247	272	141	272	10	451	69	775	592	74	561	454	104	697	564	113	542	568	345	399	579	296	326	426	416	565	346		

Table 1: Coordinate data file structure

Sample logistics (MOR: Mors) and Microscope type (LTM: Light microscope)	Slide ID and serial number	Observation code and pike on-off (1: Normal, 1: Pike-on)	Microscope stage position (X and Y)	Lens type (A: x10 and x5 zoom lens)	Comments	Microscope machine type (L3: Olympus BX40)	Scale bar length (dots)	Scale length (μm)	1 Spine length	2	3	1 Basal side length, linear mode (μm)	2	3	1 Strut length (μm)	2	3	1 Basal ring corner-strut junction (μm)	2	3	1 Basal corner-pike junction (μm)	2	3	1 Pike length (μm)	2	3	1 Basal corner angle (deg)	2	3	1 Basal-strut angle (deg)	2	3	1 Apical junction outer angle (μm)	2	3	1 Apical junction outer angle (deg)	2	3	1 Spine-basal angle (deg)	2	3	
MORLTM	1-159	1,1	0.1, 0.1	A	NO.1-159 PIKE-ON SHORT-SP	L3	57	10	10	10	6	60	62	57	20	15	19	29	32	29	34	32	28	3	2	6	64	55	60	64	55	60	80	96	80	100	122	136	152	153	148	
MORLTM	1-160	1,1	0.1, 0.1	A	NO.1-160 SHORT-SP PIKE-ON	L3	119	10	6	11	7	41	42	39	9	12	10	20	20	21	20	20	21	0	0	0	63	54	61	63	54	61	85	92	83	117	116	125 (omit)	145	142	148	
MORLTM	1-161	1,1	0.1, 0.1	A	NO.1-161 SHORT-SP PIKE-ON	L3	57	10	5	13	9	57	53	57	18	18	14	28	27	29	31	28	28	3	2	3	55	62	61	55	62	61	84	91	88	119	114	125	154	142	147	
MORLTM	1-166	1,1	0.1, 0.1	A	NO.1-166 SHORT-SP PIKE-ON	L3	106	10	3	7	4	49	55	52	14	15	14	25	28	26	25	28	26	1	0	1	65	59	54	65	59	54	90	87	86	118	118	122	157	162	153	

ID area

Morphometric result area

Table 2: Measurement data file structure

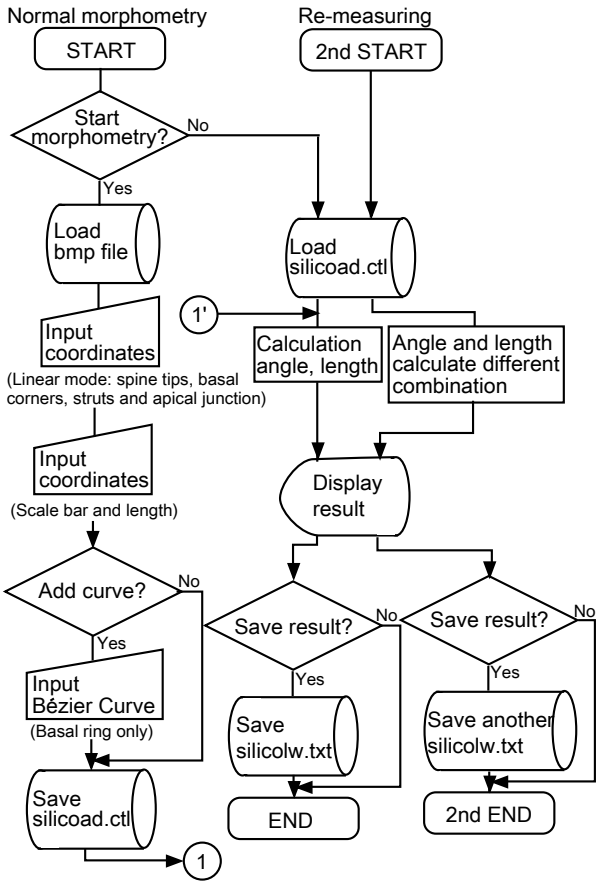

Figure 4: Morphometric program flow chart. The measurement data can be outputted from the program, and re-measurement is possible by reusing the coordinate data file

skewness, S.D. etc) was computed with SAS® Release 9.4 TS1M2 (SAS Institute, Inc., licensed by Yamagata University). A general flow chart showing all steps in the morphometric analysis is shown in Figure 4.

3. Results

The morphometric program size is 51Kbytes with no program library or plug-ins. A total of 154 *Corbisema* specimens were measured, with whorl coordinate and measurement data file sizes of 52Kbytes and 47Kbytes, respectively. A summary of the morphometric (lengths based on linear and Bézier curves) and statistical (kurtosis, skewness, standard deviation, mean and minimum/maximum) data are given in Table 3. Since all *Corbisema* skeletons are similar in shape (i.e., triangular) the data on angles between skeletal elements are not presented here.

The results of the morphometric analysis are plotted in Figure 5. The radial spine length ranges from 3–17μm with a mean length of ≈ 8μm, while the basal side length ranges from 24–79μm with a mean of ≈ 51μm. The struts range from 6–24μm with a mean length of ≈ 14μm. The distance from basal ring corner (= one apex of the triangle) to the strut attachment position on the basal side ranges

	Radial spines	Basal sides	Struts	Distance from basal corner to strut	Distance from pike to strut
Min (μm)	3	24	6	11	0
Max (μm)	17	79	24	36	4
Mean (μm)	7.9	50.9	14.4	23.8	0.7
Std dev (μm)	2.4	9.5	3	4.7	0.8
Skewness	0.45	–0.26	0.11	–0.32	1.23
Kurtosis	0.04	–0.33	–0.24	–0.44	1.72
				(N = 181)	(N = 154)

Table 3: Primary statistical summary of measurement data

from 11–36μm. Of all the specimens observed, 154 bore pikes and 27 lacked pikes. The distance from the strut to the nearest pike ranges from 0–4μm with a mean of 0.7μm.

4. Discussion

4.1 Morphometric analysis

Like most other *Corbisema* spp., the skeletons of *C. apiculata* are isosceles triangles with two equal sides (e.g., McCartney *et al*., 2014a; this study), albeit with curved basal sides, which means their overall shape is slightly circular. All the plots of element lengths (Figure 5a–b, d–e) exhibit a unimodal distribution, and thus there is no recognizable difference among the analyzed specimens based on skeletal dimensions. This could suggest that the specimens selected randomly for the analysis represent a single taxon; however, these specimens represent a mixture of pike-less and pike-bearing forms, and showed a significant distance between the strut and the nearest pike (Figure 5c, f). These differences could be viewed in two different ways with respect to silicoflagellate classification.

4.2 Pikes as taxonomically important structures

Among the three modern silicoflagellate genera, two possess pikes (*Stephanocha* and *Dictyocha*) while the other (*Octactis*) does not. From the literature and from our own observations, pike-bearing species never lose their pikes and pike-less species never gain pikes, regardless of the circumstances (cultures, aberrants, etc.). This strongly suggests that the presence or absence of pikes is fixed in the genetic blueprint of each species. Given this situation, the mixture of pike-less (15%) and pike-bearing (85%) forms in the early Eocene Mors sample could be interpreted as representing more than one taxon (see Figure 2c and 2a–b, respectively).

Furthermore, 83% of the Mors specimens bear pikes located close to the strut, while the remaining 17% of the specimens have pikes more than 1μm away from the strut (Figure 5f). Normally, pike position is a good indicator of double skeleton configuration, with pikes close to the

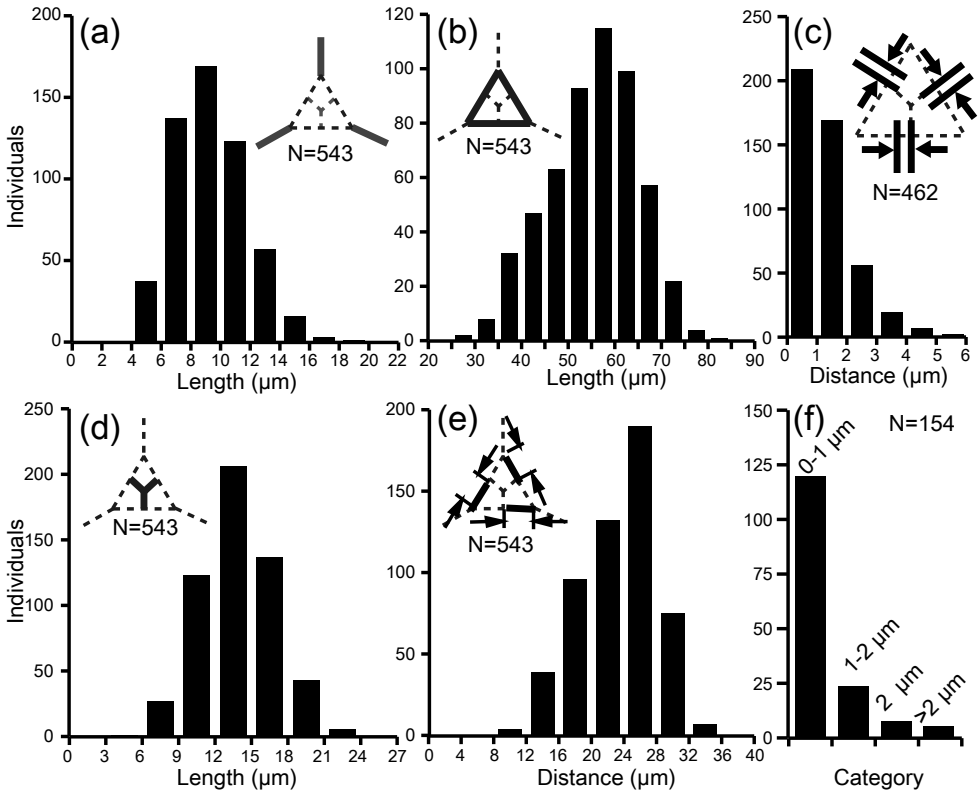

Figure 5: Histograms showing the primary measurement summary of the **(a)** radial spine length, **(b)** basal side length, **(c)** the distance from pike to strut, **(d)** strut length, **(e)** the distance from basal ring corner to strut, and **(f)** the pike-strut distance assigned to size categories

strut associated with the 'Star-of-David' configuration and those some distance away from the strut associated with the 'corner-to-corner' configuration. All modern silicoflagellates use the 'corner-to-corner' configuration, regardless of whether they possess pikes (*Stephanocha* and *Dictyocha*) or not (*Octactis*), and never switch to the 'Star-of-David' configuration, suggesting that this is genetically-controlled. In recent papers McCartney *et al*. (2014a, 2014b) proposed that different configurations represented different lineages, which would, if accepted, necessitate the formation of new genera; however, the configuration of the generitype, *C. geometrica*, is presently unknown.

4.3 Presence or absence of pikes

Silicoflagellates are currently classified using their overall skeletal shape (number of basal sides) and the presence/absence of apical ring structures. In the fossil record some genera (*Corbisema*, *Dictyocha*) contain both pike-less and pike-bearing species. At present, no genus has been erected solely on the basis of pike position and the presence/absence of pikes, and doing so would radically alter the current classification scheme. Furthermore, in this study some individual skeletons of *Corbisema apiculata* had variable pike-strut distances, which in a few cases were different by as much as 2–3μm, suggesting that the pike-strut distance may not be as significant as discussed above. In this study we averaged the pike-strut distance to reduce the effects of one 'aberrant' distance on a single skeleton (Figure 5f). This procedure still left about 3% of total specimens with a pike-strut distance of 2–5μm, which clearly separates them from the majority of specimens which had average pike-strut distances of < 1μm. Whether this is significant enough to justify separation at the species/genus level may only be answered following further morphometric studies.

4.4 Future studies

Our modified morphometric program showed that the *C. apiculata* specimens had a unimodal distribution with respect to basal side and spine lengths, but also showed that there were differences in the pike-strut distances. This story is further complicated because *C. apiculata* and *C. triacantha* are difficult to distinguish and in the literature their identification is often confused (e.g., see Loeblich *et al*., 1968, pl.23, figs 1, 10 and 11, all described as *Dictyocha triacantha* or *D. triacantha* var. *apiculata* from the Recent Pacific Ocean). In a second paper we will address this problem using the morphometric program described herein.

5. Summary

1. The main program routines, input methods and database code structures of Tsutsui (2000) were modified in order to create the 51Kbyte *Corbisema* morphometric program. The morphometric data was calculated from the two-dimensional light micrographs of *Corbisema apiculata* and is useful for supplementing morphologic descriptions and for explaining pike position distances more easily.

2. The early Eocene sample from the Fur Formation of Mors, Denmark, was chosen because (1) silicoflagellates are well preserved, (2) *Corbisema apiculata* is abundant, and (3) the sample has already yielded double skeletons in both configurations.

3. The double skeleton configurations of *Corbisema*, 'Star-of-David' and 'corner-to-corner', are a direct result of the pike positions on the skeleton pairs. The 'Star-of-David' configuration always requires the presence of pikes, which are positioned close to the base of the strut, whilst the 'corner-to-corner' configuration may be held together by organic material or pikes positioned away from the strut. In *Corbisema apiculata* we encountered pike-less and pike-bearing forms, with the pikes of the latter forms positioned either near (i.e., within 0–1μm) or away (>1μm distance) from the strut. This suggests that *C. apiculata* could produce double skeletons of either configuration, or that *C. apiculata* is a species complex containing more than one taxon.

Acknowledgements

Emeritus Professor Niichi Nishiwaki (Nara University) and Emeritus Professor Shiro Nishida (Nara University of Education) provided useful comments and discussions on fossil silicoflagellates and statistics. We are deeply grateful to Mr. Yamamoto, veteran technical engineer of Japan Maritime Self-Defense Forces, who checked the program tests, database architectures, and the program for debugging. We would also like to thank Friedel Hinz of the Friedrich Hustedt Diatom Study Centre, Alfred Wegener Institute (AWI) for providing the Mors sample used in this study. The comments and suggestions of Elisa Malinverno and an anonymous reviewer helped to improve the manuscript.

References

Aurahs, R., Treis, Y., Darling, K. & Kucera, M. 2011. A revised taxonomic and phylogenetic concept for the planktonic foraminifer species *Globigerinoides ruber* based on molecular and morphometric evidence. *Marine Micropaleontology*, **79**: 1–14.

Beaufort, L. & Dollfus, D. 2004. Automatic recognition of coccoliths by dynamical neural networks. *Marine Micropaleontology*, **51**: 57–73.

Bollmann, J., Quinn, P.S., Vela, M., Brabec, B., Brechner, S., Cortés, M.Y., Hilbrecht, H., Schmidt, D.N., Schiebel, R. & Thierstein, H.R. 2004. Automated Particle Analysis: Calcareous Microfossils. *In*: E. Francus (Ed.). *Image Analysis, Sediments and Paleoenvironments*. Springer, Dordrecht, Netherlands: 229–252.

Boney, A.D. 1976. Observations on the silicoflagellate *Dictyocha speculum* Ehrenb.: Double skeletons and mirror images. *Journal of the Marine Biological Association of the United Kingdom*, **56**: 263–266.

Chambers, L.M., Pringle, M., Fitton, G., Larsen, L.M., Pedersen, A.K. & Parrish, R. 2003. Recalibration of the Paleocene-Eocene boundary (P-E) using high precision U-Pb and Ar-Ar isotopic dating. Abstract, EGS-AGU-EUG Joint Assembly, Nice.

Chang, F.H. 2015. Cell morphology and life history of *Dictyocha octonaria* (Dictyochophyceae, Ochrophyta) from Wellington Harbour, New Zealand. *Phycological Research*: doi: 10.1111/pre.12107.

Chang, F.H., McVeagh, M., Gall, M. & Smith, P. 2012. *Chattonella globosa* is a member of Dictyochophyceae: reassignment to *Vicicitus* gen. nov., based on molecular phylogeny, pigment composition, morphology and life history. *Phycologia*, **51** (4): 403–420.

Collins, J.S.H., Schulz, B.P. & Jakobsen, S.L. 2005. First record of brachyuran decapods (Crustacea, Decapoda) from Fur Formation (early Eocene) of Mors and Fur Island, Denmark. *Bulletin of the Mizunami Fossil Museum*, **32**: 17–22.

Cortese, G. & Bjørklund, K.R. 1997. The morphometric variation of *Actinomma boreale* (Radiolaria) in Atlantic boreal waters. *Marine Micropaleontology*, **29**: 271–282.

Cortese, G. & Gersonde, R. 2007. Morphometric variability in the diatom *Fragilariopsis kerguelensis*: Implications for Southern Ocean palaeoceanography. *Earth and Planetary Science Letters*, **257**: 526–544.

Cubillos, J.C., Henderiks, J., Beaufort, L., Howard, W.R. & Hallegraeff, G.M. 2012. Reconstructing calcification in ancient coccolithophores: Individual coccolith weight and morphology of *Coccolithus pelagicus* (sensu lato). *Marine Micropaleontology*, **92–93**: 29–39.

Dollfus, D. & Beaufort, L. 1999. Fat neural network for recognition of position-normalised objects. *Neural Networks*, **12**: 553–560.

Dumitrica, P. 2014. Double skeletons of silicoflagellates: Their reciprocal position and taxonomical and paleobiological values. *Revue de Micropaléontologie*, **57**: 57–74.

Fenner, J. 1994. Diatoms of the Fur Formation, their taxonomy and biostratigraphic interpretation: Results from the Harre borehole, Denmark. *Aarhus Geoscience*, **1**: 99–163.

Forrest, A.R. 1972. Interactive interpolation and approximation by Bézier polynomials. *The Computer Journal*, **15**(1): 71–79.

Heilmann-Clausen, C., Nielsen, O.B. & Gersner, F. 1985. Lithostratigraphy and depositional environments in the Upper Paleocene and Eocene of Denmark. *Bulletin of the Geological Society of Denmark*, **33**: 287–323.

Iida, T. 2002. 99Basic Interpreter Ver. 1.19 (http://www.sagami.ne.jp/tadaka/99Basic/).

Homann, M. 1991. Die Diatomeen der Fur-Formation (Alttertiär, Limfjord/Dänemark). *Geologisches Jahrbuch, Reihe A*, **123**: 1–285.

Jordan, R.W., Abe, K. & Iwataki, M. submitted. Dictyochophyceae. *Encyclopedia of Life Sciences (eLS)*. John Wiley & Sons, Inc., New York.

Jordan, R.W. & McCartney, K. 2015. *Stephanocha* nom. nov., a replacement name for the illegitimate silicoflagellate genus *Distephanus* (Dictyochophyceae). *Phytotaxa*, **201**(3): 177–187.

Jørgensen, F., Sandersen, P.B.E., Auken, E., Lykke-Andersen, H. & Sørensen, K. 2005. Contributions to the geological mapping of Mors, Denmark – A study based on a large-scale TEM survey. *Bulletin of the Geological Society of Denmark*, **52**: 53–75.

Knappertsbusch, M.W. & Schneider, C. 2009. AMOR – A new system for automated imaging of microfossils for morphometric analyses. *Palaeontologia Electronica*, **12**: H.2, 12.2.2T

Lindbladh, M., O'Connor, R. & Jacobson, G.L., Jr. 2002. Morphometric analysis of pollen grains for paleoecological studies: Classification of *Picea* from eastern North America. *American Journal of Botany*, **89**(9): 1459–1467.

Loeblich, A.R., Loeblich, L., Tappan, H. & Loeblich, A.R., Jr. 1968. Annotated index of fossil and recent silicoflagellates and ebridians with descriptions and illustrations of validly proposed taxa. *The Geological Society of America, Inc., Memoir* **106**: 319pp.

Lohmann, G.P. 1983. Eigenshape analysis of microfossils: A general morphometric procedure for describing changes in shape. *Journal of the International Association of Mathematical Geology*, **15**: 659–672.

Malinverno, E. 2010. Extant morphotypes of *Distephanus speculum* (Silicoflagellata) from the Australian sector of the Southern Ocean: Morphology, morphometry and biogeography. *Marine Micropaleontology*, **77**: 154–174.

Marshall, S.M. 1934. The Silicoflagellata and Tintinoidea. *Great Barrier Reef Expedition 1928–29, Scientific Reports*, **4**: 623–634.

McCartney, K. 1988. SILICO: A computer program for the three-dimensional measurement of silicoflagellate skeletons. *Computers and Geosciences*, **14**(1): 99–111.

McCartney, K. & Loper, D.E. 1989. Optimized skeletal morphologies of silicoflagellate genera *Dictyocha* and *Distephanus*. *Paleobiology*, **15**: 283–298.

McCartney, K. & Loper, D.E. 1992. Optimal models of skeletal morphology for the silicoflagellate genus *Corbisema*. *Micropaleontology*, **38**: 87–93.

McCartney, K., Harwood, D.M. & Witkowski, J. 2010. A rare double skeleton of the silicoflagellate *Corbisema*. *Journal of Micropalaeontology*, **29**: 185–186.

McCartney, K., Abe, K., Witkowski, J. & Jordan, R.W. 2014a. Two rare silicoflagellate double skeletons of the Star-of-David configuration from the Eocene. *Journal of Micropalaeontology*, **34** (1): 97–99.

McCartney, K., Witkowski, J., Jordan, R.W., Daugbjerg, N., Malinverno, E., van Wezel, R., Kano, H., Abe, K., Scott, F., Schweizer, M., Young, J.R., Hallegraeff, G.M. & Shiozawa, A. 2014b. Fine structure of silicoflagellate double skeletons. *Marine Micropaleontology*, **113**: 10–19.

McCartney, K., Abe, K., Harrison, M.A., Witkowski, A., Harwood, D.M., Jordan, R.W. & Kano, H. 2015. Silicoflagellate double skeletons in the geologic record. *Marine Micropaleontology*, **117**: 65–79.

Mertens, K.N., Ribeiro, S., Bouimetarhan, I., Caner, H., Nebout, N.C., Dale, B., De Vernal, A., Ellegaard, M., Filipova, M., Godhe, A., Goubert, E., Grøsfjeld, K., Holzwarth, U., Kotthoff, U., Leroy, S.A.G., Londeix, L., Marret, F.,

Matsuoka, K., Mudie, P.J., Naudts, L., Peña-Manjarrez, J.L., Persson, A., Popescu, S.M., Pospelova, V., Sangiorgi, F., van der Meer, M.T.J., Vink, A., Zonneveld, K.A.F., Vercauteren, D., Vlassenbroeck, J. & Louwye, S. 2009. Process length variation in cysts of a dinoflagellate, *Lingulodinium machaerophorum*, in surface sediments: Investigating its potential as salinity proxy. *Marine Micropaleontology*, **70**: 54–69.

Moestrup, Ø. & Thomsen, H.A. 1990. *Dictyocha speculum* (Silicoflagellata, Dictyochophyceae), studies on armoured and unarmoured stages. *Biologiske Skrifter*, **37**: 1–57.

Nielsen, E. 1959. Eocene turtles from Denmark. *Meddelser fra Dansk Geologisk Forening*, **14**: 96–114.

Pappas, J.L. & Stoermer, E.F. 1995. Multidimensional analysis of diatom morphologic and morphometric phenotypic variation and relation to niche. *Ecoscience*, **2**(4): 357–367.

Pedersen, G.K. 1981. Anoxic events during sedimentation of a Paleogene diatomite in Denmark. *Sedimentology*, **28**: 487–504.

Pedersen, G.K. & Surlyk, F. 1983. The Fur Formation, a late Paleocene ash-bearing diatomite from northern Denmark. *Bulletin of the Geological Society of Denmark*, **32**: 43–65.

Perch-Nielsen, K. 1976. New silicoflagellates and a silicoflagellate zonation in north European Paleocene and Eocene diatomites. *Bulletin of the Geological Society of Denmark*, **25**: 27–40.

Rasband, W.S. 1997–2013. ImageJ. U. S. National Institutes of Health, Bethesda, Maryland, USA (https://imagej.nih.gov/ij/).

Schneider, C.A., Rasband, W.S. & Eliceiri, K.W. 2012. NIH Image to ImageJ: 25 years of image analysis. *Nature Methods*, **9**: 671–675.

Shiono, M. & Jordan, R.W. 1996. Recent diatoms of Lake Hibara, Fukushima Prefecture. *Diatom*, **11**: 31–63.

Siver, P.A., Wolfe, A.P., Rohlf, F.J., Shin, W. & Jo, B.Y. 2013. Combining geometric morphometrics, molecular phylogeny, and micropaleontology to assess evolutionary patterns in *Mallomonas* (Synurophyceae, Heterokontophyta). *Geobiology*, **11**: 127–138.

Tsutsui, H. 2000. Digital characterization of silicoflagellate for numerical taxonomy. *Geoinfomatics*, **11**(1): 35–42 (In Japanese with English abstract).

Tsutsui, H., Takahashi, K., Nishida, S. & Nishiwaki, N. 2009. Intraspecific morphological variation with biometry of *Distephanus speculum* (Silicoflagellata). *Marine Micropaleontology*, **72**: 239–250.

Tsutsui, H. & Takahashi, K. 2009. Biometry of *Distephanus medianoctisol* (Silicoflagellata) in the sea-ice covered environment of the central Arctic Ocean, summer 2004. *Memoire Faculty Science,* Kyushu University, Series D, *Earth and Planetary Science*, **32**(2): 57–68.

Veselá, J., Neustupa, J., Pichrtová, M. & Poulícková, A. 2009. Morphometric study of *Navicula* morphospecies (Bacillariophyta) with respect to diatom life cycle. *Fottea*, **9**(2): 307–316.

Young, J.R., Kucera, M. & Chung, H.-W. 1996. Automated biometrics on captured light microscope images of *Emiliania huxleyi*. *In*: A. Moguilevsky, & R. Whatley (Eds). *Microfossils and Oceanic Environments*. Aberystwyth-Press, Aberystwyth: 261–280.